Double ligand activation in silyl-substituted rare-earth cyclobutadienyl complexes

Article (Accepted Version)

Double Ligand Activation in Silyl-Substituted Rare-Earth Cyclobutadienyl Complexes

Anindita Chakraborty,[a] Benjamin M. Day,[a] James P. Durrant,[a,b] Mian He,[a] Jinkui Tang,*[c] Richard A. Layfield*[a]

[a] Department of Chemistry, School of Life Sciences, University of Sussex, Brighton, BN1 9QR, U.K.

[b] Department of Chemistry, School of Natural Sciences, University of Manchester, Manchester, M13 9PL, U.K.

[c] State Key Laboratory of Rare Earth Resource Utilization, Changchun Institute of Applied Chemistry, Chinese Academy of Sciences, Changchun 130022, P.R. China.

ABSTRACT: The sodium cyclobutadienyl (Cb) reagent $[Na_2\{\eta^4\text{-}C_4(SiMe_3)_4\}(THF)]_2$ (**2**) reacts with rare-earth halides $[MCl_3(THF)_x]$, where M = Y, Dy (x = 3.5) and Lu (x = 3), giving the sandwich coordination polymers $[M\{\eta^3\text{-}C_4(SiMe_3)_4H\}\{\eta^4\text{-}C_4(SiMe_3)_3\text{-}\kappa\text{-}(CH_2SiMe_2\}Na]_\infty$ (**3**$_\mathbf{M}$, M = Y, Dy, Lu). The coordination environments of the rare-earth metals in **3**$_\mathbf{M}$ feature an η^4-cyclobutadienyl ligand, with additional coordination by a tuck-in trimethylsilyl group, and an η^3-cyclobutenyl ligand. The ligand activation is thought to be a consequence of deprotonation of the Cb ligand by **2**. The axial nature of the crystal field in **3**$_\mathbf{M}$ is reflected in the single-molecule magnet properties of **3**$_\mathbf{Dy}$, which has an anisotropy barrier of 309 cm^{-1} in zero applied magnetic field.

π-Bonded aromatic ligands have played a pivotal role in the development of rare-earth organometallic chemistry. In this context, by far the most common ligand is cyclopentadienyl (Cp), the myriad derivatives of which have underpinned key milestones in rare-earth chemistry, including: alkane activation via σ-bond metathesis;[1,2] catalysis;[3,4] multiconfigurational electronic structure;[5,6] new and exotic oxidation states;[7] and high-temperature single-molecule magnets (SMMs).[8–11] Organometallic compounds containing ligands based on larger rings, particularly cyclooctatetraene (COT), have also accounted for significant advances in our understanding of the chemical and physical properties of the rare-earth elements.[12–15] In contrast, rare-earth organometallics containing the four-membered, dianionic cyclobutadienyl ring, $[Cb]^{2-}$, represent an unexplored region of chemical space and 5f derivatives are uncommon.[16] The scarcity of rare-earth Cb compounds is not hard to understand: the pro-ligands are highly strained 4π-antiaromatic cyclobutadiene rings, making them much harder to synthesize and isolate than Cp and COT pro-ligands.[17,18] Furthermore, cyclobutadienes have remarkably complex electronic structure, *viz.* the elegant studies from Sekiguchi *et al*. in which it was shown that 1,2,3,4-*tetrakis*(trimethylsilyl)cyclobuta-1,3-diene, $C_4(SiMe_3)_4$, is converted into a triplet diradical form on heating.[19]

To date, the only structurally authenticated rare-earth cyclobutadienyl compounds are the coordination polymers $[\{K_2(\eta^6\text{-toluene})\}M\{\eta^4\text{-}C_4(SiMe_3)_4\}\{\eta^4\text{-}C_4(SiMe_3)_3\text{-}\kappa\text{-}(CH_2SiMe_2\}]_\infty$ (M = Dy, **1**$_\mathbf{Dy}$; M = Y, **1**$_\mathbf{Y}$), which form by dint of potassium cations bridging between the η^4-$C_4(SiMe_3)_4$ ligands and deprotonated trimethylsilyl substituents.[20] Although these compounds contain *bis*(η^4-cyclobutadienyl)metal units, the activated trimethylsilyl substituent, which adopts a tuck-in bonding mode, is problematic since it precludes isolation of the originally targeted sandwich complexes $[M\{\eta^4\text{-}C_4(SiMe_3)_4\}_2]^-$, the terbium and dysprosium versions of which will very likely show excellent SMM properties. The origins of the tuck-in bond in **1**$_\mathbf{M}$ seemingly lie within the Brønsted basicity of $K_2[C_4(SiMe_3)_4]$, which may be involved in the deprotonation of $[M\{\eta^4\text{-}C_4(SiMe_3)_4\}^2]^-$ *in situ*, as witnessed by the formation of the potassium cyclobutenyl by-product $[(\eta^6\text{-toluene})K\{\eta^3\text{-}C_4(SiMe_3)_4H]$.

In the light of these previous observations, we were interested in probing the role of the alkali metal in salt metathesis reactions of cyclobutadienyl anions with rare-earth halides. We therefore synthesized the sodium salt of $[C_4(SiMe_3)_4]^{2-}$ (Cb"") and investigated its reactions with $[MCl_3(THF)_x]$ with M = Y, Dy (x = 3.5) and Lu (x = 3), which proceed according to Scheme 1.

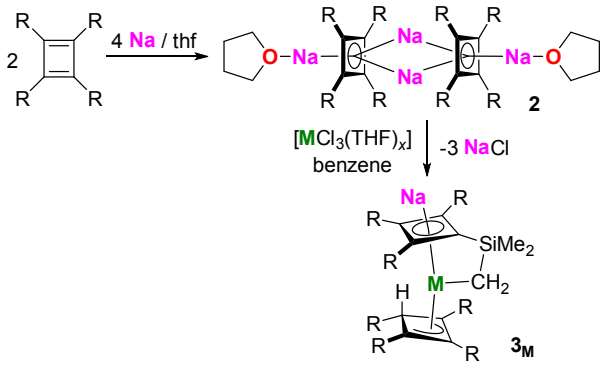

Scheme 1. Synthesis of **2** and **3M** with R = $SiMe_3$ and M = Y, Dy (x = 3.5) and Lu (x = 3).

The pro-ligand 1,2,3,4-*tetrakis*(trimethylsilyl)cyclobuta-1,3-diene was synthesized according to a modified version of a literature procedure,[17] and the subsequent reaction with a slight excess of sodium metal gave $[Na_2\{\eta^4\text{-}C_4(SiMe_3)_4\}(THF)]_2$ (**2**) in an isolated crystalline yield of 72%. Placing **2** under vacuum for a few hours results in partial loss of THF. The molecular structure of **2**, which was revealed by X-ray diffraction, consists of dimeric molecules in which two Cb"" ligands each coordinate to three sodium atoms (Figure 1). Two disordered sodium atoms, Na(2) and Na(3), bridge between the Cb"" ligands via slipped η^4-interactions, with the trimethylsilyl substituents oriented in a manner consistent with the presence of C–H···Na interactions, similar to those observed in the monomeric structure of Li_2(Cb"").[17] The two ends of the structure of **2** are capped by η^4-Cb"" coordination to Na(1) and Na(1A), each of which is also bound to a THF ligand. For the bridging sodium atoms, the Na–C and Na–Cb"" centroid distances are 2.634(2)-3.039(19) Å and 2.962(18)/2.589(2) Å, respectively, whereas the analogous distances to the terminal sodium atoms are 2.539(15) Å and 2.311(2) Å, respectively. The ^{1}H, ^{13}C and ^{29}Si NMR spectra are consistent with the solid-state structure (Figures S1-S3).

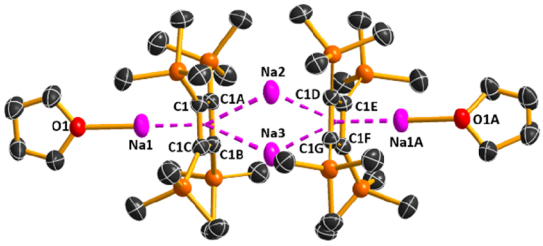

Figure 1. Thermal ellipsoid representation (50% probability) of the molecular structure of **2**. For clarity, the hydrogen atoms are not shown.

Before attempting reactions of **2** with rare-earth halides, the stability of the reagent in benzene and toluene was investigated by ^{1}H NMR spectroscopy. Under reflux, compound **2** is stable in benzene for at least 12 hours (Figure S4); it is also stable in refluxing toluene for approximately one hour, however heating for longer periods results in changes to the ^{1}H NMR spectrum and formation of an amorphous red precipitate (Figure S5). For comparative purposes, K_2Cb"" was also studied under the same conditions and found to decompose in toluene (Figures S6, S7); the reaction with toluene led to the isolation of a few crystals of benzyl-potassium,[21] supporting the notion that K_2Cb"" is a strong Brønsted base. This observation suggests that the red precipitate involved in the reaction of toluene with **2** is benzyl-sodium. The use of alkali metal salts of cyclobutadienyl dianions therefore requires a careful choice of solvent to avoid unwanted side reactions.

The reactions of $[MCl_3(THF)_x]$ with **2** were carried out in refluxing benzene for 16 hours, followed by recrystallization of the crude products in benzene or toluene at –40°C. X-ray diffraction revealed the products to be isostructural coordination polymers based on repeats units with the formula $[M\{\eta^3\text{-}C_4(SiMe_3)_4H\}\{\eta^4\text{-}C_4(SiMe_3)_3\text{-}\kappa\text{-}\{CH_2SiMe_2\}Na]_\infty$ (**3M**, M = Y, Dy, Lu, Figures 2, S8, S9). In the repeat unit, the rare-earth metal is complexed by an η^4-Cb"" ligand in which a trimethylsilyl substituent has been deprotonated and engages in a tuck-in interaction. The second ligand bound to the rare-earth metal is a protonated version of the cyclobutadienyl ligand, which adopts an η^3-cyclobutenyl coordination mode. The η^4-Cb"" ligand also bridges to a sodium cation, which then bridges to another tuck-in carbon atom on an adjacent repeat unit, resulting in propagation of the polymer. Pertinent geometric parameters for **3Dy** include Dy–C distances of 2.506(11)-2.571(11) Å to the η^4-Cb"" ligand and Dy(1)–C(2), Dy(1)–C(3) and Dy(1)–C(4) distances of 2.582(12), 2.744(11) and 2.617(10) to the η^3-Cb"" ligand. The Dy–C(9) distance to the tuck-in carbon is 2.494(12) Å. The distances from dysprosium to the centroids of the η^4-Cb"" and η^3-Cb"" ligands are 2.308(5) and 2.460(5) Å, respectively, and the Cb-Dy-Cb angle is 159.157(5)°. The Na–C distances to the η^4-Cb"" ligand are in the range 2.503(12)-2.895(11) Å and the Na–C distance to the tuck-in carbon of an adjacent unit of **3Dy** is 2.689(13) Å. Similar distributions of geometric parameters are found in the structures of **3Y** and **3Lu** (Tables S1, S2).

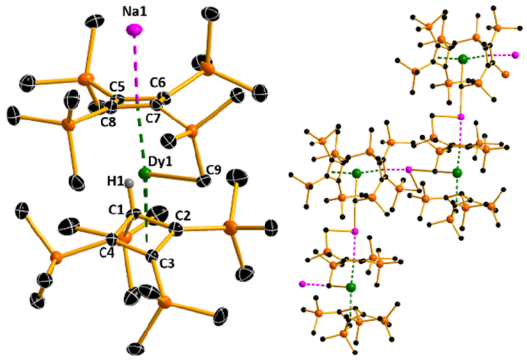

Figure 2. Thermal ellipsoid representation (30% probability) of: (a) the molecular structure of **3Dy**, and; (b) a segment of the extended polymeric structure. For clarity, the hydrogen atoms are not shown.

The ^{1}H and ^{13}C NMR spectra of **3Y** (Figures S10-S13) and **3Lu** (Figures S14-S20), recorded in toluene-D_8/THF-D_8

(3:1) solvent mixtures, are consistent with the solid-state structures, with each displaying eight resonances in the region $\delta(^{13}C)$ = 0-10 ppm for the trimethylsilyl carbon atoms, a resonance at 48.6 ppm (**3**$_{Y}$) and 50.3 ppm (**3**$_{Lu}$) for the protonated carbon atom of the η^3-cyclobutenyl ring, and five resonances in the region 105-125 ppm for the η^4-cyclobutadienyl and η^3-cyclobutenyl carbon atoms.

The fate of the Cb"" ligands during the synthesis of **3**$_{M}$ illustrates that the Cb ring can itself undergo activation (protonation) in addition to the trimethylsilyl substituents. In **1**$_{M}$, deprotonation of the trimethylsilyl substituent was the only observed activation mode; however, given the reactivity of K_2Cb"" towards toluene, the participation of the solvent in these reactions cannot be ruled out. In the synthesis of **3**$_{M}$, since Na_2Cb"" does not react with benzene, the ligand activation processes are presumably a consequence of Cb coordination to the rare-earth metal. A possible sequence that accounts for the formation of **3**$_{M}$ is proposed in Scheme 2. In the first step, displacement of two chloride ligands from the rare-earth metal by one [Cb""]$^{2-}$ ligand can be envisaged, resulting in a putative intermediate with

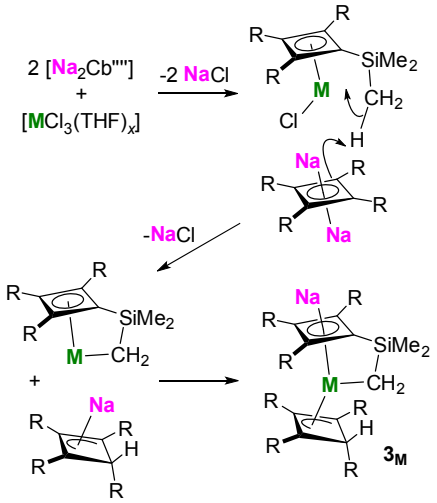

Scheme 2. A possible mechanism accounting for the formation of compound **3**$_{M}$.

composition [(Cb"")MCl]. Subsequently, a second equivalent of Na_2Cb"" may deprotonate a trimethylsilyl substituent to give an intermediate tuck-in complex and the cyclobutenyl-sodium species [Na{η^3-C_4(SiMe$_3$)$_4$H}], which then adds to the tuck-in intermediate to give **3**$_{M}$. Whilst the actual mechanism through which **3**$_{M}$ forms is likely to be more complicated, the sequence in Scheme 2 at least provides some insight into the reactivity of the cyclobutadienyl ligand, which contrasts to that of other carbocyclic ligands in rare-earth chemistry.

In addition to the reactivity, we were also intrigued by the potential impact of the double ligand activation mode on the dynamic magnetic properties of **3**$_{Dy}$. Since the discovery of dysprosium metallocene SMMs, the organometallic approach to enhancing the magnetic blocking temperature (T_B) and the effective energy barrier to reversal of the magnetization (the anisotropy barrier, U_{eff}) has grown to be a fruitful area of research.[8,22,23] The basic principles governing the design of dysprosium sandwich SMMs invoke molecular geometries in which two approximately *trans*-disposed ligands generate a strong axial crystal field by virtue of a small-but-significant covalent contribution to the dysprosium-ligand bonding.[24–27] When the crystal field is strong *and* highly axial, T_B and U_{eff} can be very large; however, when a competing equatorial crystal field is introduced, the opposite effect is observed and fast relaxation occurs within the magnetic ground state, typically via quantum tunnelling of the magnetization (QTM). These principles were demonstrated through a study of **1**$_{Dy}$, which shows slow relaxation in zero applied D.C. magnetic field, although the QTM is strong and an anisotropy barrier could not be determined.[20] In an applied field of 1 kOe, a barrier of U_{eff} = 325 cm^{-1} was measured. The poor SMM properties of **1**$_{Dy}$ are consistent with the dominant influence of the equatorial tuck-in [CH_2SiMe_2Cb]$^-$ ligand despite the strong axial crystal field provided by the cyclobutadienyl ligands.

The magnetic properties of **3**$_{Dy}$ were measured on a polycrystalline sample restrained in eicosane. The temperature-dependence of the molar magnetic susceptibility, *i.e.* $\chi_M T(T)$, was measured in a DC field of 1 kOe, and the field-dependence of the magnetization, *i.e.* $M(H)$, was measured at fields in the range 0-7 T at 2, 3 and 5 K, and the results are typical of a compound containing a Dy^{3+} ion with a $^6H_{15/2}$ ground term.[28] Full details of these measurements are provided in the Supporting Information (Figures S21-S22). Dynamic-field magnetic susceptibility measurements on **3**$_{Dy}$ reveal typical SMM behaviour in zero applied DC field, with well-defined maxima in the frequency-dependence of the out-of-phase susceptibility, $\chi''(\nu)$, in the temperature range 1.9-37 K (Figures 3, S23-S26).

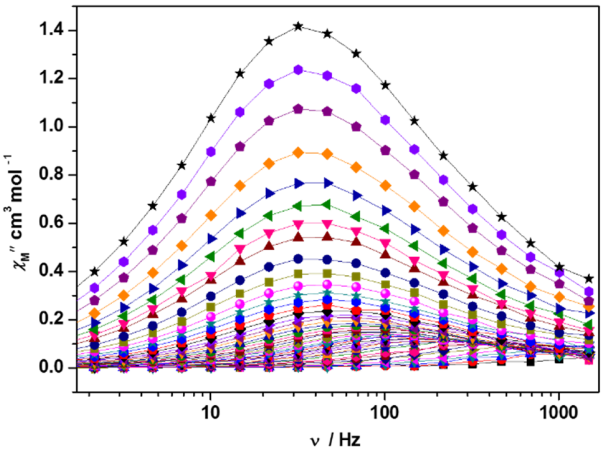

Figure 3. Frequency dependence of the out-of-phase molar magnetic susceptibility (χ''_M) for **3**$_{Dy}$, collected in zero D.C. field at A.C. frequencies of ν = 0.1-1488 Hz at 1.9 K (black stars), 2.2 K (lilac hexagons), 2.5-5 K in 0.5 K intervals, and then 6-40 K in 1 K intervals. Solid lines represent a guide for the eye.

From the AC susceptibility data, the magnetic relaxation times (τ) were extracted using a standard Cole-Cole fitting procedure with α-parameters in the range 0.05-

0.28, which indicates a moderate distribution of relaxation times (Figures S27-S30, Table S3). A plot of ln (τ/s) versus T^{-1} revealed that the relaxation in **3$_{Dy}$** is dominated by thermally activated processes above approximately 12 K (Figure S31), followed by a curved section that may reflect Raman relaxation, and at lower temperatures τ is only weakly temperature-dependent, indicating the dominance of QTM. Fitting the data with the standard equation $\tau^{-1} = \tau_0^{-1}e^{-U_{eff}/k_BT} + CT^n + \tau_{QTM}^{-1}$, in which C and n are the Raman coefficient and Raman exponent, respectively, and τ_{QTM}^{-1} is the rate of QTM yielded U_{eff} = 309(20) cm^{-1}, τ_0 = 1.03(4) × 10^{-9} s, C = 0.78(2) s^{-1} K^{-n}, n = 2.07(8) and τ_{QTM} = 3.78(8) × 10^{-3} s. The extracted barrier for **3$_{Dy}$** is similar to that determined for **1$_{Dy}$**, however it is notable that the barrier for **3$_{Dy}$** was determined in zero applied magnetic field, suggesting that the competing equatorial crystal field in this doubly activated cyclobutadienyl complex is less influential than the equatorial crystal field in its singly activated analogue.

In conclusion, the sodium cyclobutadienyl reagent [Na$_2${η^4-C$_4$(SiMe$_3$)$_4$}(THF)]$_2$ (**2**) reacts with rare-earth halides accompanied by a previously unseen double ligand activation process, which results in the tuck-in/allyl sandwich compounds [M{η^3-C$_4$(SiMe$_3$)$_4$H}{η^4-C$_4$(SiMe$_3$)$_3$-κ-(CH$_2$SiMe$_2$}Na]$_\infty$ (**3$_M$**) with M = Y, Dy and Lu. Our working hypothesis is that the ligand activation modes in **3$_M$** are a consequence of the basicity of **2** combined with the C–H acidity of the trimethylsilyl substituents, which may be enhanced upon coordination to the rare-earth metals. The axial nature of the crystal field in **3$_{Dy}$** was confirmed by the observation of SMM behaviour in zero applied magnetic field, with an associated anisotropy barrier of 309 cm^{-1}. Alternative synthetic approaches to the intact transfer of η^4-Cb ligands to rare-earth elements are under development in our laboratory.

ASSOCIATED CONTENT

Supporting Information

Synthesis details, analytical characterization including X-ray crystallography and CIF files, magnetic property measurements. This material is available free of charge via the Internet at http://pubs.acs.org.

AUTHOR INFORMATION

Corresponding Author

* R.Layfield@sussex.ac.uk

Notes

The authors declare no competing financial interest.

ACKNOWLEDGMENT

AC thanks the Royal Society and the Science and Engineering Research Board (India) for a Newton Advanced Fellowship (NF170539). JT and RAL thank the Royal Society for a Newton Advanced Fellowship (NA160075). RAL also thanks the ERC (CoG 646740) and the EPSRC (EP/M022064/1) for support.

REFERENCES

(1) Watson, P. L. Methane Exchange Reactions of Lanthanide and Early-Transition-Metal Methyl Complexes. *J. Am. Chem. Soc.* **1983**, *1* (12), 6491–6493. https://doi.org/10.1021/ja00359a023.

(2) Thompson, M. E.; Baxter, S. M.; Bulls, A. R.; Burger, B. J.; Nolan, M. C.; Santarsiero, B. D.; Schaefer, W. P.; Bercaw, J. E. "s-Bond Metathesis" for C-H Bonds of Hydrocarbons and Sc-R (R = H, Alkyl, Aryl) Bonds of Permethylscandocene Derivatives. Evidence for Noninvolvement of the 7r System in Electrophilic Activation of Aromatic and Vinylic C-H Bonds. *J. Am. Chem. Soc* **1987**, No. 3, 203–219.

(3) Allouche, F.; Chan, K. W.; Fedorov, A.; Andersen, R. A.; Copéret, C. Silica-Supported Pentamethylcyclopentadienyl Ytterbium(II) and Samarium(II) Sites: Ultrahigh Molecular Weight Polyethylene without Co-Catalyst. *Angew. Chemie* **2018**, *130* (13), 3489–3492. https://doi.org/10.1002/ange.201800542.

(4) Nishiura, M.; Guo, F.; Hou, Z. Half-Sandwich Rare-Earth-Catalyzed Olefin Polymerization, Carbometalation, and Hydroarylation. *Acc. Chem. Res.* **2015**, *48* (8), 2209–2220. https://doi.org/10.1021/acs.accounts.5b00219.

(5) Schultz, M.; Burns, C. J.; Schwartz, D. J.; Andersen, R. A. Solid-State Structures of Base-Free Ytterbocenes and Inclusion Compounds of Bis(Pentamethylcyclopentadienyl)Ytterbium with Neutral Carboranes and Toluene: The Role of Intermolecular Contacts. *Organometallics* **2000**, *19* (5), 781–789. https://doi.org/10.1021/om990821g.

(6) Berg, D. J.; Boncella, J. M.; Andersen, R. A. Preparation of Coordination Compounds of Cp*2Yb with Heterocyclic Nitrogen Bases: Examples of Antiferromagnetic Exchange Coupling across Bridging Ligands. *Organometallics* **2002**, *21* (22), 4622–4631. https://doi.org/10.1021/om020477e.

(7) Evans, W. J. Tutorial on the Role of Cyclopentadienyl Ligands in the Discovery of Molecular Complexes of the Rare-Earth and Actinide Metals in New Oxidation States. *Organometallics* **2016**, *35* (18), 3088–3100. https://doi.org/10.1021/acs.organomet.6b00466.

(8) Guo, F.-S.; Day, B. M.; Chen, Y.-C.; Tong, M.-L.; Mansikkamäki, A.; Layfield, R. A. Magnetic Hysteresis up to 80 Kelvin in a Dysprosium Metallocene Single-Molecule Magnet. *Science (80-.).* **2018**, *362* (6421), 1400–1403. https://doi.org/10.1126/science.aav0652.

(9) Randall McClain, K.; Gould, C. A.; Chakarawet, K.; Teat, S. J.; Groshens, T. J.; Long, J. R.; Harvey, B. G. High-Temperature Magnetic Blocking and Magneto-Structural Correlations in a Series of Dysprosium(Iii) Metallocenium Single-Molecule Magnets. *Chem. Sci.* **2018**, *9* (45), 8492–8503. https://doi.org/10.1039/C8SC03907K.

(10) Guo, F.-S.; Day, B. M.; Chen, Y.-C.; Tong, M.-L.; Mansikkamäki, A.; Layfield, R. A. A Dysprosium Metallocene Single-Molecule Magnet Functioning at the Axial Limit. *Angew. Chemie - Int. Ed.* **2017**, *56* (38). https://doi.org/10.1002/anie.201705426.

(11) Goodwin, C. A. P.; Ortu, F.; Reta, D.; Chilton, N. F.; Mills, D. P. Molecular Magnetic Hysteresis at 60 Kelvin in Dysprosocenium. *Nature* **2017**, *548*, 439.

(12) Xémard, M.; Zimmer, S.; Cordier, M.; Goudy, V.; Ricard, L.; Clavaguéra, C.; Nocton, G. Lanthanidocenes: Synthesis, Structure, and Bonding of Linear Sandwich Complexes of Lanthanides. *J. Am. Chem. Soc.* **2018**, *140* (43), 14433–14439. https://doi.org/10.1021/jacs.8b09081.

(13) Mooßen, O.; Dolg, M. Two Interpretations of the Cerocene Electronic Ground State. *Chem. Phys. Lett.* **2014**, *594*, 47–50. https://doi.org/10.1016/j.cplett.2014.01.022.

(14) Cloke, F. G. N.; Green, J. C.; Kilpatrick, A. F. R.; O'Hare, D. Bonding in Pentalene Complexes and Their Recent Applications. *Coord. Chem. Rev.* **2017**, *344*, 238–262. https://doi.org/10.1016/j.ccr.2016.12.006.

(15) Münzfeld, L.; Schoo, C.; Bestgen, S.; Moreno-Pineda, E.; Köppe, R.; Ruben, M.; Roesky, P. W. Synthesis, Structures and Magnetic Properties of [(H9-C9H9)Ln(H8-C8H8)] Super Sandwich Complexes. *Nat. Commun.* **2019**, *10* (1), 3135. https://doi.org/10.1038/s41467-019-10976-6.

(16) Liddle, S.; Boronski, J.; Doyle, L.; Seed, J.; Wooles, A. F-Element Half-Sandwich Complexes: A Tetrasilylcyclobutadienyl-Uranium(IV)-Tris(Tetrahydroborate) Anion Pianostool Complex. *Angew.*

Chemie Int. Ed. **2019**, doi.org/10.1002/anie.201913640.

(17) Sekiguchi, A.; Matsuo, T.; Watanabe, H. Synthesis and Characterization of a Cyclobutadiene Dianion Dilithium Salt: Evidence for Aromaticity. *J. Am. Chem. Soc.* **2000**, *122* (23), 5652–5653. https://doi.org/10.1021/ja0004175.

(18) Sekiguchi, A.; Matsuo, T. Doubly Charged Four-Membered Ring Systems: Cyclobutadiene Dianions and Heavy Cyclobutadiene Dianions. *Synlett* **2006**, *2006* (17), 2683–2698. https://doi.org/10.1055/s-2006-950280.

(19) Kostenko, A.; Tumanskii, B.; Kobayashi, Y.; Nakamoto, M.; Sekiguchi, A.; Apeloig, Y. Spectroscopic Observation of the Triplet Diradical State of a Cyclobutadiene. *Angew. Chemie Int. Ed.* **2017**, *56* (34), 10183–10187. https://doi.org/10.1002/anie.201705228.

(20) Day, B. M.; Guo, F.-S.; Giblin, S. R.; Sekiguchi, A.; Mansikkamäki, A.; Layfield, R. A. Rare-Earth Cyclobutadienyl Sandwich Complexes: Synthesis, Structure and Dynamic Magnetic Properties. *Chem. - A Eur. J.* **2018**, *24* (63), 16779–16782. https://doi.org/10.1002/chem.201804776.

(21) Unkelbach, C.; O'Shea, D. F.; Strohmann, C. Insights into the Metalation of Benzene and Toluene by Schlosser's Base: A Superbasic Cluster Comprising PhK, PhLi, and TBuOLi. *Angew. Chemie Int. Ed.* **2014**, *53* (2), 553–556. https://doi.org/10.1002/anie.201306884.

(22) Day, B. M.; Guo, F.-S.; Layfield, R. A. Cyclopentadienyl Ligands in Lanthanide Single-Molecule Magnets: One Ring To Rule Them All? *Acc. Chem. Res.* **2018**, *51* (8), 1880–1889. https://doi.org/10.1021/acs.accounts.8b00270.

(23) Chen, S.-M.; Xiong, J.; Zhang, Y.-Q.; Yuan, Q.; Wang, B.-W.; Gao, S. A Soft Phosphorus Atom to "Harden" an Erbium(Iii) Single-Ion Magnet. *Chem. Sci.* **2018**, *9* (38), 7540–7545. https://doi.org/10.1039/C8SC01626G.

(24) Ungur, L.; Chibotaru, L. F. Strategies toward High-Temperature Lanthanide-Based Single-Molecule Magnets. *Inorg. Chem.* **2016**, *55* (20), 10043–10056. https://doi.org/10.1021/acs.inorgchem.6b01353.

(25) Zhu, Z.; Guo, M.; Li, X.-L.; Tang, J. Molecular Magnetism of Lanthanide: Advances and Perspectives. *Coord. Chem. Rev.* **2019**, *378*, 350–364. https://doi.org/10.1016/J.CCR.2017.10.030.

(26) Liu, J.-L.; Chen, Y.-C.; Tong, M.-L. Symmetry Strategies for High Performance Lanthanide-Based Single-Molecule Magnets. *Chem. Soc. Rev.* **2018**, *47* (7), 2431–2453. https://doi.org/10.1039/C7CS00266A.

(27) Escalera-Moreno, L.; Baldoví, J. J.; Gaita-Ariño, A.; Coronado, E. Exploring the High-Temperature Frontier in Molecular Nanomagnets: From Lanthanides to Actinides. *Inorg. Chem.* **2019**, *58* (18), 11883–11892. https://doi.org/10.1021/acs.inorgchem.9b01610.

(28) Benelli, C.; Gatteschi, D. Magic Dysprosium. In *Introduction to Molecular Magnetism*; John Wiley & Sons, Ltd, 2015; pp 277–294. https://doi.org/10.1002/9783527690541.ch16.

Graphic entry for the Table of Contents (TOC).